Journal of Applied Fluid Mechanics, Vol. 17, No. 1, pp. 148-158, 2024.
Available online at www.jafmonline.net, ISSN 1735-3572, EISSN 1735-3645.
https://doi.org/10.47176/jafm.17.1.1999

Structural Design and Performance Study of a Reciprocating Vortex Ring Generator

M. L. Zhou, D. Han†, L. Zhu, S. Y. Yu, Y. F. Gao, Q. L. Shi and W. F. He

College of Energy and Power Engineering, Nanjing University of Aeronautics and Astronautics, Nanjing, 210016, Jiangsu, China

†*Corresponding Author Email: handong@nuaa.edu.cn*

ABSTRACT

Vortex rings can maintain their structure during motion and achieve long-distance transport with low energy consumption, which is a fluid transport method with great energy-saving potential. In this paper, a reciprocating vortex ring generator structure is designed, which can generate two vortex rings during the reciprocating motion of one piston, making full use of the thrust in the reciprocating motion period of the piston and improving the vortex ring generation frequency compared with traditional vortex ring generators. For the characteristics of long-distance transport of vortex rings, an experimental platform is designed and built, and 277 sets of experiments are carried out with different geometric parameters. The results show that the effect of generating two vortex rings could be achieved under other parameter conditions, except for some parameter conditions where the diameter ratio $D_1/D_2 = 4$. By analyzing the influence of baffle width ratio, length ratio, and diameter ratio on the moving distance of vortex rings, the performance of the vortex ring generator is preliminarily studied. In 277 sets of experiments, the maximum moving distance ratio x_1 of vortex ring 1 is 13.7 when $L_1/L_2 = 2.4$, $D_1/D_2 = 2$, and $w_1 = 0.2$. And the maximum moving distance ratio x_2 of vortex ring 2 is 20 when $L_1/L_2 = 2$, $D_1/D_2 = 2.5$, and $w_2 = 0.2$.

Article History

Received May 10, 2023
Revised August 28, 2023
Accepted September 3, 2023
Available online November 1, 2023

Keywords:

Vortex ring generator
Structural design
Moving distance
Piston
Fluid transport

1. INTRODUCTION

Vortex ring is a self-propelled three-dimensional ring structure (Dasouqi et al., 2020), which is widely found in transmission of human blood (Saaid et al., 2018), volcanic eruptions (Taddeucci et al., 2021), and the propulsive motion of living creatures such as jellyfish (Gemmell et al., 2015). Vortex rings can maintain their structure during motion and achieve long-distance transport with low energy consumption (Xiang et al., 2018). The study of vortex rings has always been a classic topic in the field of fluid mechanics (Ren et al., 2016). Through numerical simulation and experimental research, the structure of vortex rings (Shadden et al., 2006; Noro et al., 2013), vortex ring collisions (Nguyen et al., 2019; New et al., 2020), and other physical characteristics have been studied. In addition, the theoretical formulas for vortex rings have also been proposed (Krueger, 2008; Buttà & Marchioro, 2020).

With the rapid economic and social development (Yu et al., 2023), the demand for a comfortable living environment is getting higher (Tan et al., 2023). Vortex ring ventilation (VRV) is a new type of air supply system consisting of vortex rings. Compared with an air supply jet (Sakhri et al., 2021), vortex rings can reduce the loss of fresh air during transportation because of their stable structures (Cao et al., 2022). Air vortex ring personalized air supply is a form of air supply with potential application for long-distance, directional, and efficient air supply to the target area (Wang et al., 2020). Zhai et al. (2022) conducted research on personalized air supply scenarios under non-isothermal conditions, exploring the impact of thermal buoyancy on the vortex ring air supply process, and proposed methods to reduce temperature difference losses. Ultimately, they found that the vortex ring air supply method has better directionality and lower attenuation rate. The vortex ring ventilation system is still in the research stage, while the effect of structural changes of the vortex ring generator on the vortex ring moving distance is less studied.

Vortex rings can be used in numerous other fields in addition to the air supply field. Mouallem et al. (2021) proposed a conceptual model for directed particle transfer using controllable vortex ring reconnection, in which

NOMENCLATURE

D_1	diameter of the outer tube	W_2	width of the inner ring baffle
D_2	diameter of the inner tube	W_3	width of the ring piston
D_3	diameter of the inlet	w_1	width ratio of the outer ring baffle
L_1	length of the outer tube	w_2	width ratio of the inner ring baffle
L_2	length of the inner tube	X_1	moving distance of vortex ring 1
S	stroke of the ring piston	X_2	moving distance of vortex ring 2
T	time of the piston forward (return) process	x_1	moving distance ratio of vortex ring 1
t	time	x_2	moving distance ratio of vortex ring 2
W_1	width of the outer ring baffle		

entrained particles can be effectively transported within the core region of the vortex ring through self-induction; Wang & Covington (2023) designed a simple vortex ring based single user olfactory display, which is a digital device that provides users with controllable odors; Vortex rings can also be applied to flow mixing in fields such as combustion engineering. In order to improve jet and mixing rates, Xia et al. (2021) combined vortex rings with swirls to enhance the intensity of turbulent fluctuations. Jain et al. (2023) studied the interaction between vortex rings and applied it to the cleaning mechanism of oily porous surfaces.

Vortex ring generators play a decisive role in vortex ring generation effect. Most of the current vortex ring generators are mechanical piston type and synthetic jet type (Ikhlaq et al., 2022), among which the mechanical piston type is the most commonly used and effective. This mechanism for generating vortex rings has also been used to study the characteristics of vortex rings (Dabiri & Gharib, 2004; Zhang et al., 2020). Maxworthy (1977) and Pullin (1979) used the piston device to generate vortex rings and studied the evolution of vortex rings. They found that the shear force caused the fluid flowing out of the piston unit to form a vortex ring. Gharib et al. (1998) conducted experiments on vortex rings in waters using a piston device, and the results showed that the volume of the vortex ring does not increase indefinitely with increasing piston thrust. When the piston thrust increases to a fixed threshold, the volume of the vortex ring itself will no longer change, and the extra volume of fluid due to the excess thrust will form the wake of the vortex ring. Dipendra et al. (2020) proposed a device and method for generating gusts in the form of vortex rings under laboratory conditions and analyzed the flow characteristics of vortex rings. The device has an unlimited range of usage and can generate continuous gusts in any direction. It can also be used to study the gust effects of natural aircraft, artificial micro air vehicles, swimmers, and aquatic plants. Limbourg and Nedić (2021b) conducted an experimental study on the vortex ring generation effect of two piston type vortex ring generators with different outlets. The experimental results showed that the vortex ring generated by the orifice outlet was better in momentum and impulse than the tube outlet; Tian et al. (2021) designed a continuous jet vortex ring generator for air supply, which mainly includes annular and conical outlets. Seth et al. (2017) designed a vortex ring generator for use in water, mainly for research in the field of biomimetics. Many scholars have changed the structure of vortex ring generators to get a better vortex ring production effect (Xia & Zhang, 2018; Limbourg et al., 2021a), but overall, the structure of the mechanical piston-type vortex ring generator is still relatively single. Only one vortex ring can be generated during a reciprocating piston movement cycle, and the thrust during the piston movement cycle cannot be fully utilized. To apply vortex rings to more fluid transport applications, it is necessary to increase the frequency of ring generation and make vortex rings move longer distances.

In this paper, a new reciprocating vortex ring generator is designed, which can effectively utilize the thrust during the reciprocating motion of the piston and increase the frequency of vortex ring generation. And the difference in the diameter of the inner and outer tubes of the generator forms a contraction channel to accelerate the second vortex ring, thus moving a long distance. In addition, considering the application of vortex rings, research is conducted on the characteristics of long-distance transportation of vortex rings, exploring the impact of geometric factors on the vortex ring moving distance (the distance from the vortex ring generation to the time when it is slow moving and about to break). In order to conduct the above research, an air vortex ring generation system was also designed and constructed.

2. STRUCTURAL DESIGN OF THE RECIPROCATING VORTEX RING GENERATOR

The structure of the reciprocating vortex ring generator designed is shown in Fig. 1. The vortex ring generator mainly consists of an outer tube, an inner tube, a ring piston, a ring baffle, a support structure, and a connection structure. The annular outlet 1 is formed between the inner and outer tubes, and the inner tube outlet is outlet 2. A ring baffle is placed at each outlet. A circular inlet on the side wall of the outer pipe connects it to the external pipe so that it can enter the fluid, the bottom of the outer pipe is sealed. The connection structure connects the ring piston to the external driving part so that the piston can move back and forth between the two tubes. The support is used to hold the inner tube inside the outer tube.

The two-dimensional vortex ring generator's working diagram is shown in Fig. 2, and the arrows in the figure indicate the direction of fluid flow. In Fig. 2(a), the ring piston starts moving from the bottom of the inner tube and moves forward rapidly to compress the fluid between the two tubes, generating the first vortex ring (vortex ring 1) at outlet 1. In Fig. 2(b), when the piston returns rapidly to the bottom of the inner tube, it will compress the fluid between the two tubes and at the rear of the outer tube to finally generate a second vortex ring (vortex ring 2) at outlet 2. The fluid is further accelerated in the compression

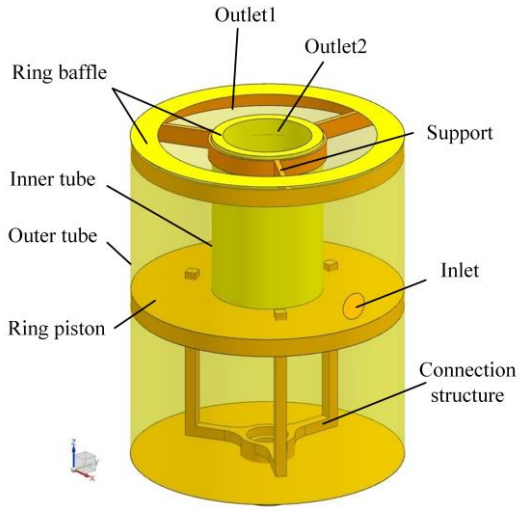

Fig. 1 Structure diagram of the reciprocating vortex ring generator

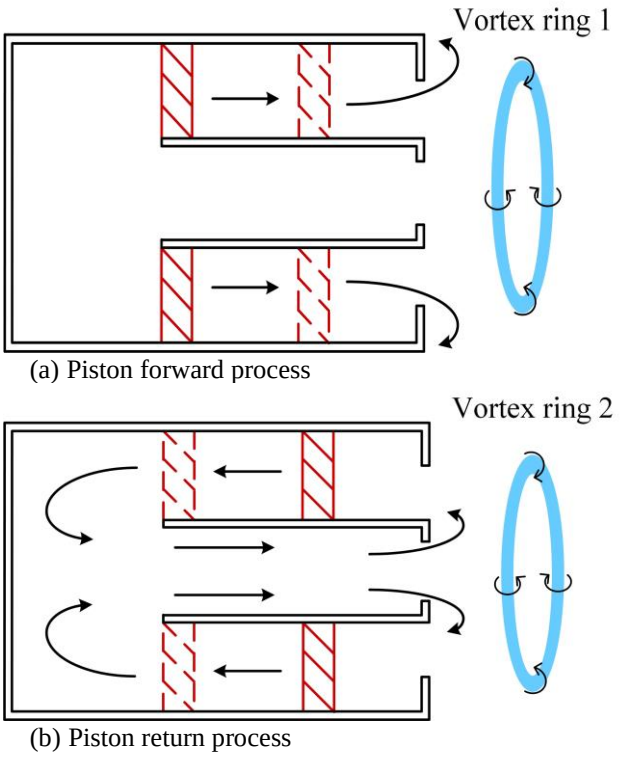

(a) Piston forward process

(b) Piston return process

Fig. 2 Structure diagram of the reciprocating vortex ring generator

process by the contraction channel created by the inner and outer tubes, causing the vortex ring 2 to move faster and farther. In this way, two vortex rings can be formed during the reciprocating motion period of the piston, making full use of the thrust of the piston.

Figure 3 shows the basic structure of the vortex ring generator, where L_1 is the length of the outer tube, L_2 is the length of the inner tube, D_1 is the diameter of the outer tube, D_2 is the diameter of the inner tube, D_3 is the diameter of the inlet, W_1 is the width of the outer ring baffle, W_2 is the width of the inner ring baffle, W_3 is the width of the ring piston.

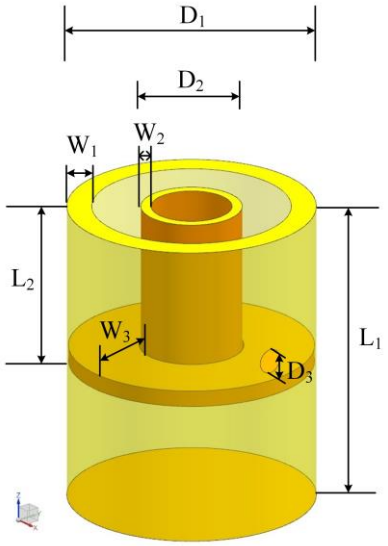

Fig. 3 Basic geometric dimensions of the reciprocating vortex ring generator

Table 1 Initial parameters of the vortex ring generator

Parameters	Value
L_1(length of the outer tube)	18cm
D_1(diameter of the outer tube)	15cm
D_3 (diameter of the inlet)	1.2cm
S (stroke of the ring piston)	7cm
T (time of the piston forward (return) process)	0.1s

The width of the ring piston W_3 varies with the diameter of the inner and outer tubes as follows：

$$W_3 = (D_1 - D_2)/2 \quad (1)$$

Define the ratio of inner and outer baffle widths as w_1 and w_2:

$$w_1 = 2W_1/D_1 \quad (2)$$

$$w_2 = 2W_2/D_2 \quad (3)$$

The dimensions of the outer tube were kept constant and the dimensions of the inner tube and the baffles were changed for different sets of experiments. Table 1 shows some initial parameters of the vortex ring generator.

3. EXPERIMENTS AND METHODS

3.1 Experimental system

The whole experimental system consists of four main parts: the driving part, the visualization part, the vortex ring generation part, and the distance measurement part.

As shown in Fig. 4, the driving part mainly includes an air compressor, a controller, a solenoid valve, and a cylinder. The visualization part includes a fan, a throttle valve, and a gasholder. The vortex ring generation part is the reciprocating vortex ring generator designed in this paper. The distance measuring part includes a side scale, two ground scales, and a camera. Figure 5 shows the physical diagram of the experimental system.

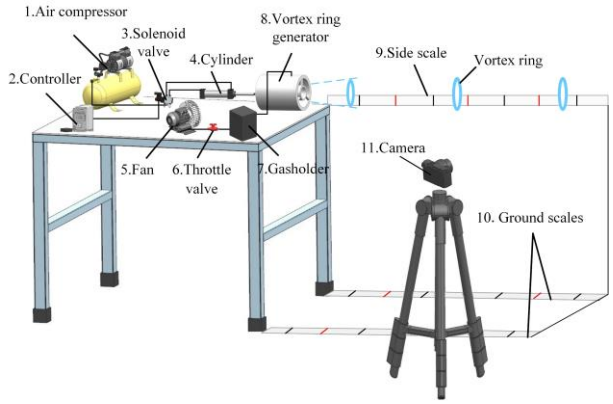

Fig. 4 Schematic diagram of the experimental system

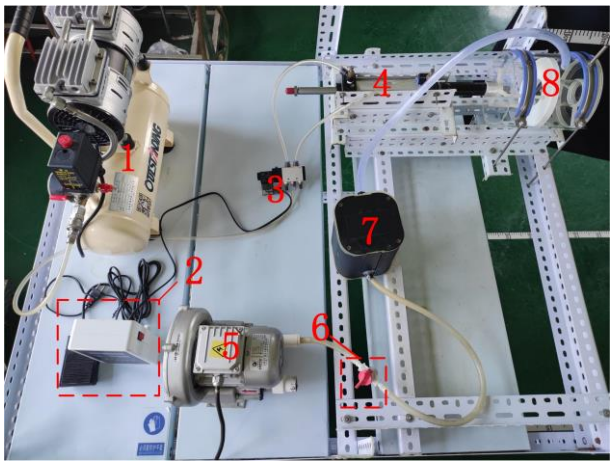

(a) The driving, the visualization, and the vortex ring generation parts

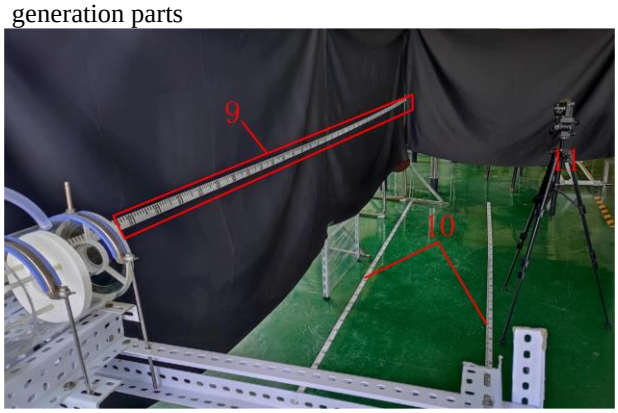

(b) The distance measurement part

Fig. 5. Physical diagram of the experimental system.

3.2 Experimental Methods

Through the solenoid valve, the air compressor delivers compressed air to the cylinder after compressing a specific volume of air. The controller controls the switch of the solenoid valve. By adjusting the cylinder's valve, compressed air enters the cylinder through the solenoid valve and pushes the cylinder rod a certain distance. The cylinder rod drives the connected vortex generator's ring piston to reciprocate, and the movement stroke of the piston remains unchanged. Ignite smoke cakes in the gasholder to produce smoke with a similar air density before the piston begins to move. Turn on the fan to make the smoke in the gasholder enter the vortex ring generator through the pipe. The throttle valve can control the flow rate of the smoke, and the appropriate flow rate can make the smoke enter the vortex ring generator more evenly to achieve a better visualization effect. The piston moves forward rapidly and compresses the smoke to generate vortex ring 1. Measure the vortex ring 1's moving distance X_1 when it is about to break. When the piston returns rapidly, vortex ring 2 is generated. Also, measure its moving distance X_2 from generation to breaking. Vortex rings may deviate during its movement, so some scales are installed on the side of the vortex ring's movement path and the ground, and a camera is used to record the vortex ring's movement process to assist in measurement.

Define the moving distance ratios of vortex ring 1 and vortex ring 2 as x_1 and x_2:

$$x_1 = X_1/L_1 \tag{4}$$

$$x_2 = X_2/L_1 \tag{5}$$

Where L_1 is the outer tube's length of the reciprocating vortex ring generator, X_1 is the moving distance of vortex ring 1, and X_2 is the moving distance of vortex ring 2.

3.3 Analysis of Errors

With a measurement accuracy of 1 cm, the experiment's main source of error is the distance measurement error. During the movement of the vortex ring, it will be affected by the flow field in the measurement area. At the same time, because the smoke density is greater than the density of air, the vortex ring may shift during the movement, which will bring measurement errors. When there are two or more vortex rings in the measurement area, each vortex ring may interact with the others and also affect the measurement of moving distances.

The flow field in the measuring area must be kept as steady as possible during each group of experiments in order to minimize measurement errors. Additionally, measurement scales should set on the side and the ground. Two people conduct the experiment; one person performs the experimental operation, and the other person measures the distance. Each experimental group should be run at least ten times, and values with large deviations should be ignored. The average of stable values should be used to calculate the ultimate vortex ring movement distance. The next vortex ring is generated when each vortex ring is about to break, reducing the interaction between the vortex rings when determining the movement distance of each vortex ring. In addition, due to the errors in human eye measurement, a camera is used to record the movement process of vortex rings, achieving the impact of auxiliary measurement.

3.4 Experimental Content

Under the same external conditions, changing the structure of the vortex ring generator can make vortex rings move at different distances. Generally, the faster the vortex ring moves, the farther it moves. Therefore, the transport characteristics of the vortex ring generator are preliminarily studied by exploring the influence of geometric factors on the moving distance of vortex rings. In this experiment, the smoke is compressed by the

Table 2 Geometric dimensions

L_1/ L_2	D_1/ D_2	w_1	w_2
1.8	2	0.1, 0.15, 0.2, 0.25, 0.3	0.1, 0.2, 0.3, 0.4, 0.5
1.8	3	0.1, 0.15, 0.2, 0.25, 0.3	0.1, 0.2, 0.3, 0.4, 0.5
1.8	4	0.1, 0.15, 0.2, 0.25, 0.3	0.1, 0.2, 0.3, 0.4, 0.5
2.4	3	0.1, 0.15, 0.2, 0.25, 0.3	0.1, 0.2, 0.3, 0.4, 0.5

reciprocating piston, and the outlet is suddenly narrowed due to the existence of a ring baffle, thus forming a vortex ring structure. The generation effect of vortex rings can be altered by changing the size of the ring baffles as well as the relative length and diameter of the inner and outer tubes. Therefore, the influence of the above factors will be studied.

Firstly, the influence of baffle width ratios on vortex ring moving distances is investigated, and the range of geometric dimensions is shown in Table 2. The value range of w_1 is between 0.1 and 0.3, and the value range of w_2 is between 0.1 and 0.5. Different L_1/L_2 and D_1/D_2 values are selected for 100 sets of experiments.

Based on the analysis of the results of the above experiments, preserve the more meaningful ranges of w_1 and w_2 to reduce repetitive work, and then carry out experiments to investigate the influence of other factors. As shown in Table 3, the range of L_1/L_2 is between 1.8 and 2.6, and the range of D_1/D_2 is between 2 and 4. Different w_1 and w_2 values are selected for 177 sets of experiments.

Table 3 Geometric dimensions after reducing the range of w_1 and w_2

L_1/ L_2	D_1/ D_2	w_1	w_2
1.8	2.5	0.15, 0.2, 0.25	0.1, 0.2, 0.3
1.8	3.5	0.2, 0.25, 0.3	0.1, 0.2, 0.3
2.4	2, 2.5	0.15, 0.2, 0.25	0.1, 0.2, 0.3
2.4	3.5	0.2, 0.25, 0.3	0.1, 0.2, 0.3
2.4	4	0.2, 0.25, 0.3	0.1, 0.2
2.0, 2.2, 2.6	2, 2.5	0.15, 0.2, 0.25	0.1, 0.2, 0.3
2.0, 2.2, 2.6	3, 3.5	0.2, 0.25, 0.3	0.1, 0.2, 0.3
2.0, 2.2, 2.6	4	0.2, 0.25, 0.3	0.1, 0.2

Based on the 100 experiments in Table 2, a total of 277 experiments will be conducted.

4. RESULTS AND ANALYSIS

4.1 Vortex Ring Generation Effect

Figure 6 shows the generation of vortex rings from two different outlets, where vortex ring 1 and vortex ring 2 are shown in red solid and red dashed frames, respectively. When t=0.5s, the piston rapidly moves forward to generate vortex ring 1 at outlet 1. At this time, the piston is stationary, and vortex ring 1 moves forward for some distance. The structure and movement of vortex ring 1 can be seen clearly between 1.0s and 4.0s. When t=7.5s, the piston quickly returns and generates vortex ring 2 at outlet 2. It is evident from the figure that vortex ring 2 flows more quickly because of the contraction channel created by the inner and outer tubes. The reciprocating vortex ring generator designed is capable of generating two vortex rings in one piston motion cycle.

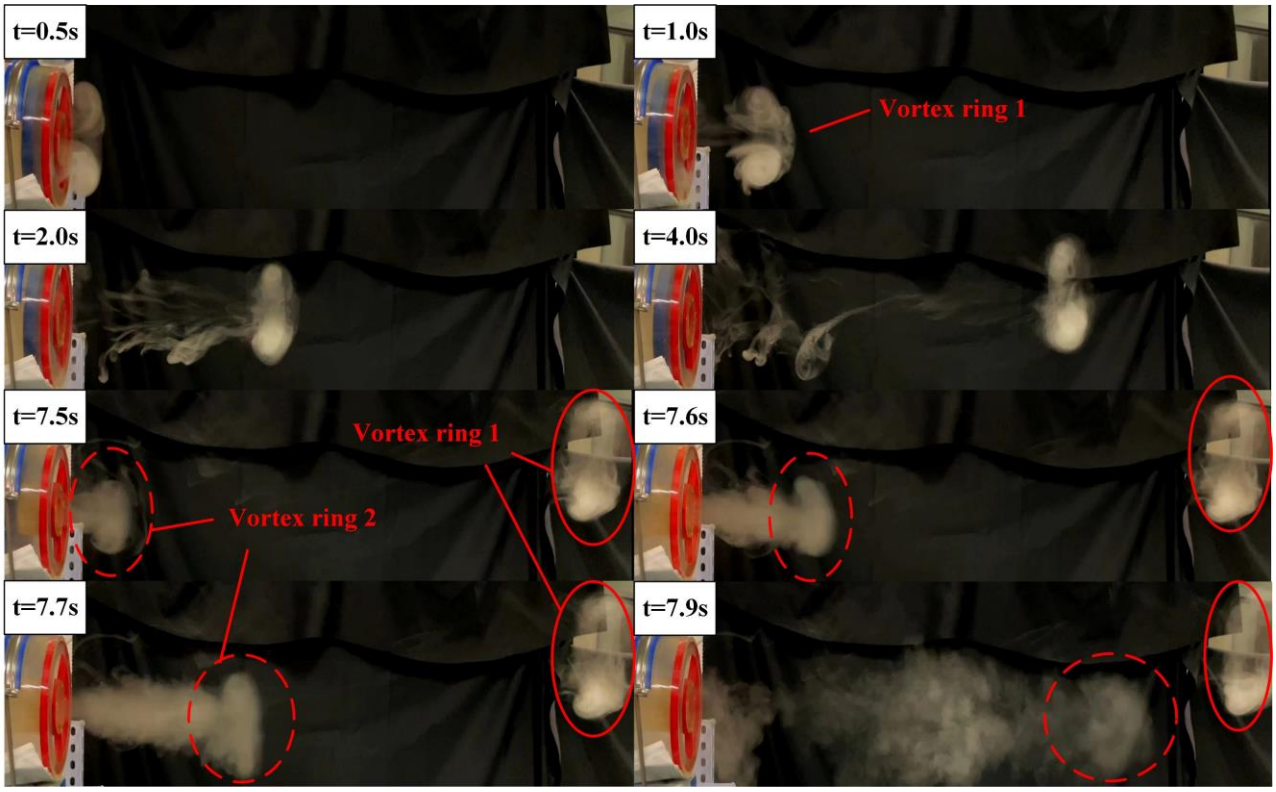

Fig. 6 Visualization of vortex rings

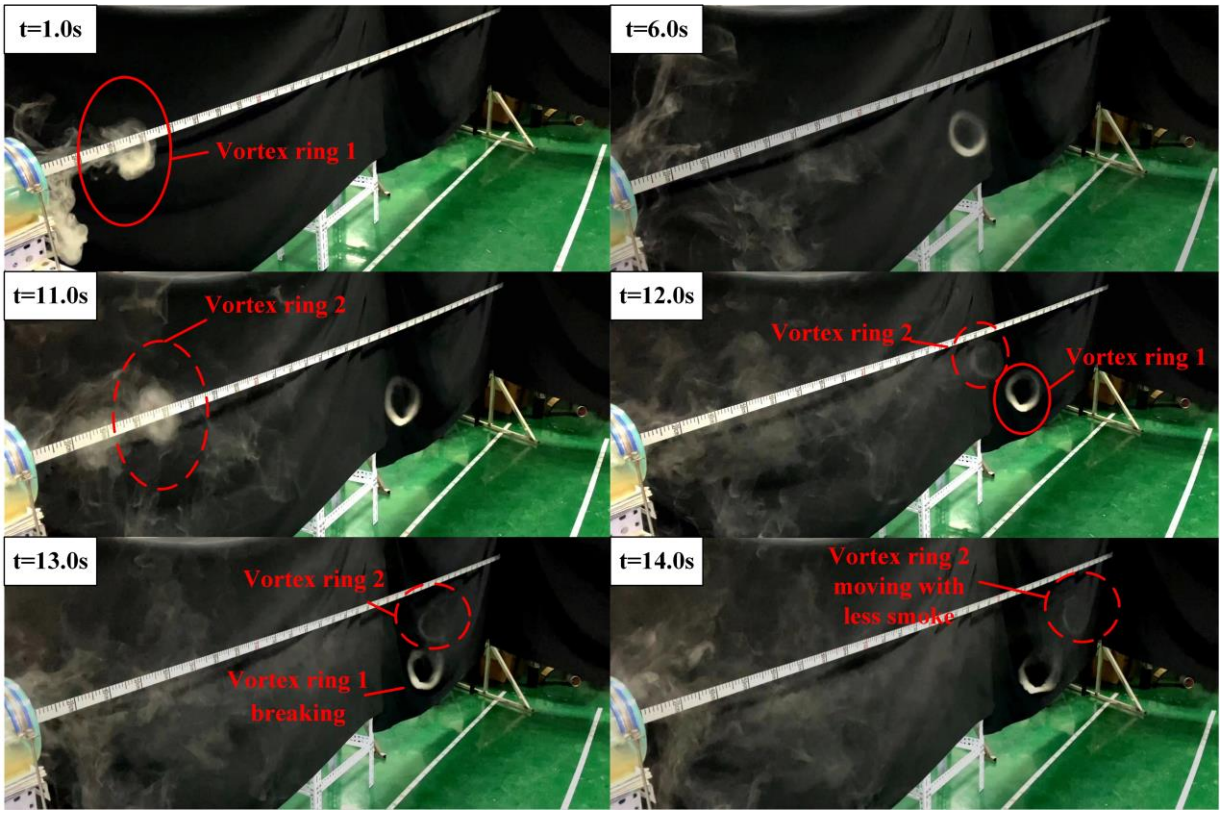

Fig. 7 Measurement process of vortex ring moving distances

Figure 7 shows the measurement process of vortex ring moving distances during experiments, and vortex ring 1 and vortex ring 2 are shown in red solid and red dashed frames respectively. Vortex ring 1 is completely generated at time t = 1.0s and is then allowed to move forward for a distance. When t = 11.0s, vortex ring 1 moves slowly. At this time, vortex ring 2 is generated and moves forward quickly. Record the distance as X1 when vortex ring 1 starts to break at t = 13.0s. Then vortex ring 2 continues to move forward carrying less amount of smoke. When vortex ring 2 begins to break, record its moving distance as X_2. Throughout the experiment, x_1 reaches maximum value of 13.7 when $L_1/L_2 = 2.4$, $D_1/D_2 = 2$ and $w_1 = 0.2$, while x_2 reaches the maximum value of 20 when $L_1/L_2 = 2$, $D_1/D_2 = 2$ and $w_2 = 0.2$.

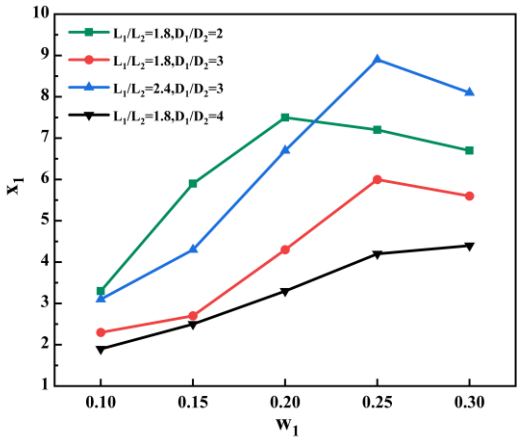

Fig. 8 Effect of w_1 on x_1

4.2 Effect of Baffle Width Ratio

A ring baffle is placed at the vortex ring generator's outlet to cause a sudden shrinkage of the outlet section. This makes the fluid accelerate as it rushes out, which is more conducive to the formation of the vortex ring structure. The acceleration will be insufficient if the baffle size is too small, and it will result in a significant local loss if the baffle size is too large. Therefore, it is necessary to conduct experimental research to investigate how baffles affect vortex ring development. A total of 100 sets of experiments were carried out, as shown in Table 2. Only the effect of w_1 on x_1 and w_2 on x_2 will be examined in the following analysis because, in the structure of the vortex ring generator designed in this paper, vortex ring 1 and vortex ring 2 are generated at the outlet 1 and outlet 2, respectively.

Figure 8 shows the effect of w_1 on x_1 under different conditions. When w_1 is small, there is insufficient fluid acceleration at the exit, which results in low vortex ring 1 velocity as well as a small moving distance x_1. However, increasing w_1 will also increase the local loss of fluid at the outlet, and when the local loss is too large, it will offset the acceleration of fluid at the outlet, so when D_1/D_2 is between 2 and 3, x_1 first increases and then decreases with the increase of w_1. When $D_1/D_2 = 2$, the difference between the inner and outer tube diameters is smaller than that of $D_1/D_2 = 3$, which means that the section of outlet 1 at $D_1/D_2 = 2$ is smaller than that at $D_1/D_2 = 3$, so x_1 peaks earlier and reaches the maximum at $w_1 = 0.2$. When $D_1/D_2 = 3$, x_1 reaches the maximum at $w_1 = 0.25$. When $D_1/D_2 = 4$, the difference between the inner and outer tube diameters

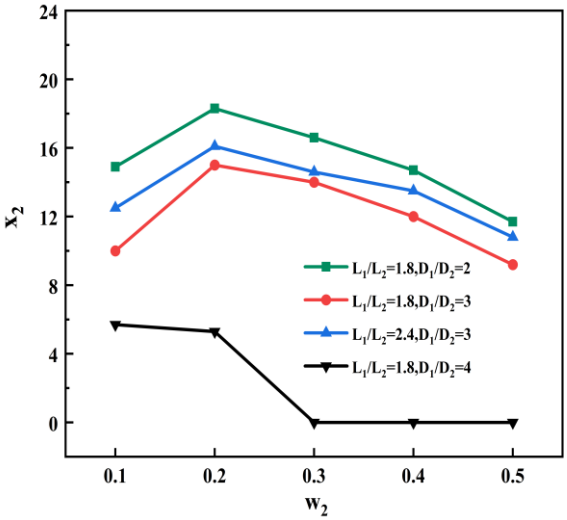

Fig. 9 Effect of w_2 on x_2

makes the section of outlet 1 larger, so x_1 keeps increasing in the taken range of w_1, but the increase is slow when $w_1 > 0.25$.

Figure 9 shows the effect of w_2 on x_2 under different conditions. The increase of the baffle width ratio w_2 makes the fluid accelerate at outlet 2 but also increases the local loss at there. Therefore, when D_1/D_2 is between 2 and 3, x_2 first increases and then decreases with the increase of w_2, peaking at $w_2 = 0.2$. The inner tube's diameter is too small compared to the outer tube when $D_1/D_2 = 4$, which causes less fluid to be compressed into the inner tube during the piston's return. However, at the same length, the small diameter of the pipe makes the loss along the flow of the fluid occupy the main influence. As a result, in this case, the local loss increases as w_2 increases, but the fluid acceleration effect is insufficient, causing x_2 to trend downward. When $w_2 \geq 0.3$, vortex ring 2 can no longer be produced, which means that $x_2 = 0$. The effect of D_1/D_2 on the moving distance will be analyzed in detail below.

4.3 Effect of Length Ratio

The length ratio L_1/L_2 mainly affects the fluid loss along the way during the generation of vortex rings and the amount of fluid compressed during the piston's reciprocating motion. The increase of L_1/L_2 is equivalent to the reduction of the inner tube's length, which will reduce the loss along the way during the generation of vortex rings. The piston will compress less fluid when it moves forward and less fluid will be conveyed by the vortex ring 1 because the inner tube's length reduction will result in a smaller cavity between the inner and outer tubes. The shorter inner tube also results in more space at the rear of the outer tube, which causes the piston to compress the fluid more when it returns and reduces the acceleration effect during the generation of vortex ring 2. One vortex ring will move a short distance if it carries too much fluid. When there is too little fluid, the fluid carried by the vortex ring structure quickly diffuses into the external environment, making vortex rings break quickly and move a short distance.

In Fig. 10, the solid line represents x_1. Under different conditions, x_1 first increases and then decreases with the increase of L_1/L_2. When $D_1/D_2 = 2$ in Fig. 10 (a), x_1 peaks at $L_1/L_2 = 2.4$, while in other cases x_1 peaks at $L_1/L_2 = 2.2$. The fluid loss along the way and the fluid carrying capacity of vortex ring 1 are decreased with an increase in L_1/L_2. As a result, the moving distance ratio x_1 increases. However, when L_1/L_2 reaches a certain point, vortex ring 1's fluid-carrying capacity is insufficient. The final result is a short moving distance as the fluid carried by vortex ring 1 quickly diffuses into the outer environment.

The dashed line in Fig. 10 represents the moving distance ratio x_2 of vortex ring 2. In most cases, x_2 is greater than x_1 because the generation process accelerates vortex ring 2 due to the difference in inner and outer tube diameters. Except for the case in Fig. 10(e), x_2 first increases and then decreases with the increase of L_1/L_2 and peaks at $L_1/L_2 = 2.0$ in all other conditions. At the beginning of the increase of L_1/L_2, the decrease of fluid loss along the way will make x_2 increase. However, when L_1/L_2 increases to a certain level, the piston will compress a large amount of fluid during the return process, weaking the acceleration effect and making the vortex ring 2 move slowly and x_2 decrease.

In the case of $D_1/D_2 = 4$ in Fig. 10 (e), because the inner tube diameter is too small, the space between the inner and outer tubes and the rear of the outer tube is too large. In this way, a large amount of fluid will be compressed during the piston return process, but very little of that fluid can be compressed into the inner tube. As a result, the generation effect of vortex ring 2 is poor and x_2 is smaller than x_1. When $L_1/L_2 \geq 2.4$ and $w_2 \geq 0.2$, vortex ring 2 can no longer be formed, and result in $x_2 = 0$.

From this, it can be seen that when $D_1/D_2 = 4$, the generation effect of vortex rings, especially vortex ring 2, is very poor, making it difficult to achieve the expected effect of the reciprocating vortex ring generator designed in this paper.

4.4 Effect of diameter ratio

The influence of the baffle ratio and length ratio on the moving distance of vortex rings have been analyzed in this paper, and the influence of the diameter ratio is analyzed in this section. The inner tube diameter will decrease as D_1/D_2 increases, which will increase the volume of the cavity between the inner and outer tubes. As a result, the piston will compress more fluid during reciprocating motion, which will directly affect the vortex ring 1 generation. As the diameter difference between the inner and outer tubes increases, the acceleration effect will also increase theoretically. However, a too-small inner tube will have less fluid compressed inside of it, which will have an impact on the vortex ring 2 generation. This makes the effect of D_1/D_2 on vortex ring 2 highly complicated and requires analysis based on data.

As shown in Fig. 11 (a), when $w_1 = 0.2$, x_1 decreases with the increase of D_1/D_2. According to the analysis of Fig. 8, when $D_1/D_2 \geq 3$, x_1 peaks at $w_1 = 0.25$, and when $D_1/D_2 < 3$, x_1 peaks at $w_1 = 0.2$, so in Fig. 11(b)

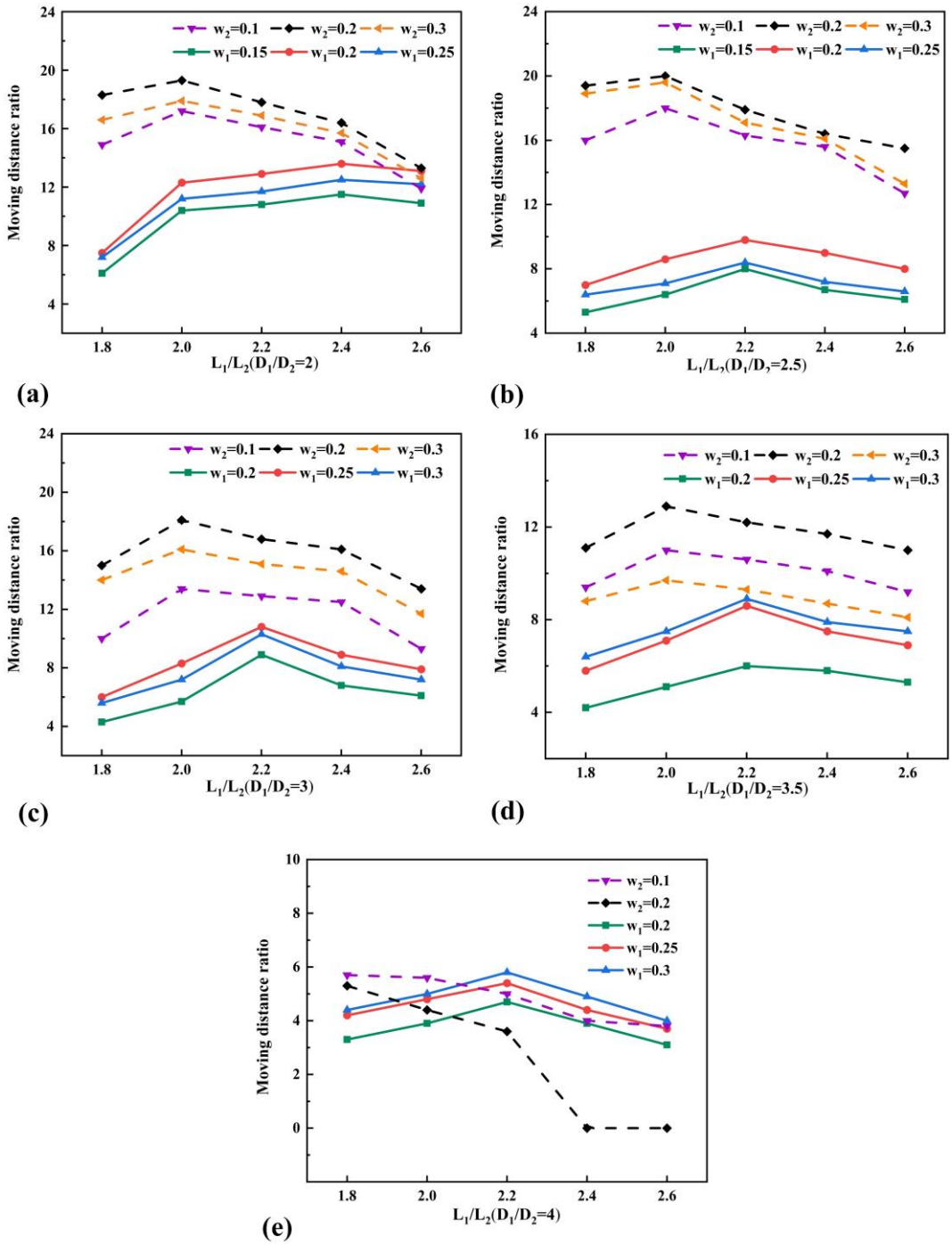

Fig. 10 Effect of L_1/L_2 on moving distance ratio, where the solid line represents x_1 and the dashed line represents x_2. (a) Under D_1/D_2 = 2, (b) Under D_1/D_2 = 2.5, (c) Under D_1/D_2 = 3, (d) Under D_1/D_2 = 3.5, (e) Under D_1/D_2 = 4

there will be an upward trend of x_1. If the whole trend in Fig. 11 (b) is divided into D_1/D_2 = 2-2.5 and D_1/D_2 = 3-4 for observation, the trend will be the same as that in Fig. 11 (a), that is, x_1 decreases with the increase of D_1/D_2. Because the loss along the way increases as the inner tube's length increases, x_1 is relatively small when L_1/L_2 = 1.8. The conclusion here corresponds to the analysis of Fig. 10.

Figure 12 shows the effect of D_1/D_2 on x_2. In several different cases, x_2 first increases and then decreases with the increase of D_1/D_2 and peaks at D_1/D_2 = 2.5. The increase of D_1/D_2 is equivalent to a decrease in the inner tube diameter. Theoretically, the acceleration effect caused by the difference in inner and outer tube diameters increases, but it also results in more fluid being compressed as the piston returns. The combined effect causes the above trend in x_2. The inner tube diameter is excessively small compared to the outer tube when D_1/D_2 = 4, which results in insufficient fluid being pushed into the inner tube and a poor generation effect of vortex ring 2. From the analysis of Fig. 10, it can be seen that the piston compresses more fluid in the return process when L_1/L_2 increases, and the local loss gradually increases as w_2 increases. This leads to the situation of x_2 = 0 in Fig. 12(b), which means that vortex ring 2 cannot be generated.

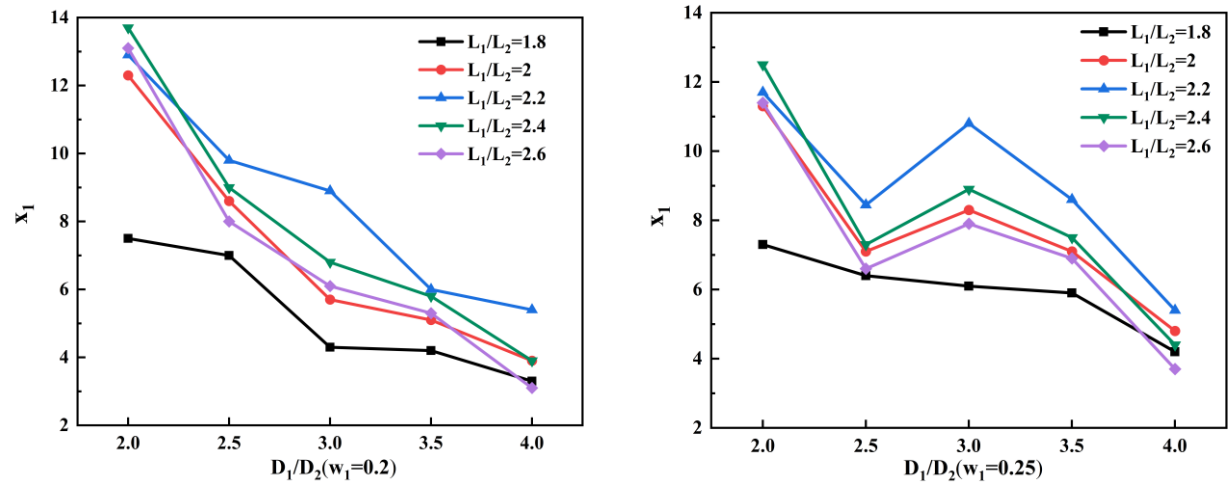

(a) Under $w_1 = 0.2$ (b) Under $w_1 = 0.25$

Fig. 11 Effect of D_1/D_2 on X_1

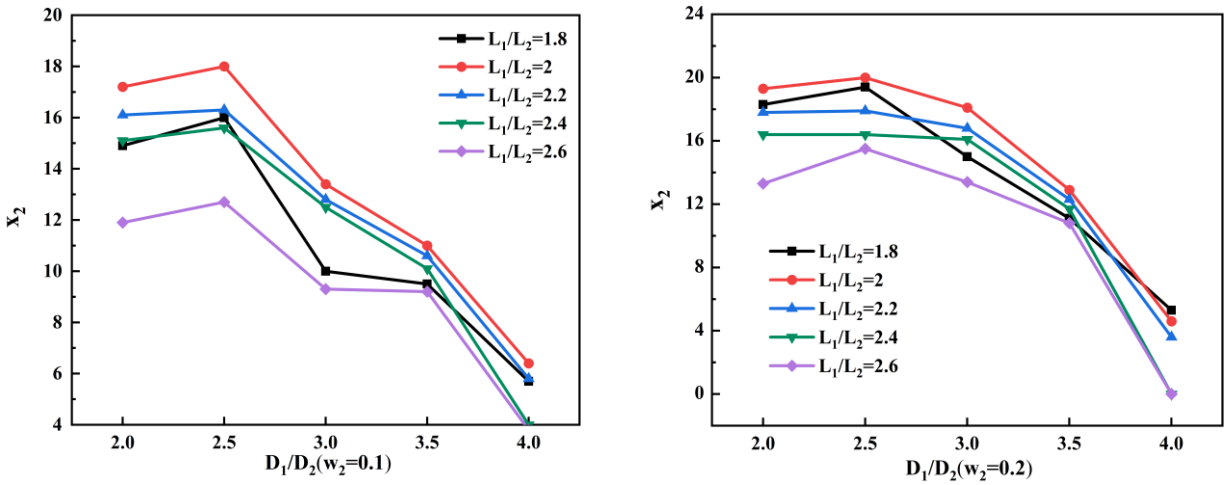

(a) Under $w_2 = 0.1$ (b) Under $w_2 = 0.2$

Fig. 12 Effect of D_1/D_2 on X_2

4. CONCLUSION

In this paper, a reciprocating vortex ring generator structure is designed, which can generate two vortex rings during the reciprocating motion of one piston relative to traditional structures. An experimental platform is designed and built to investigate the influence of geometric factors on the vortex ring moving distance. The main conclusions are as follows:

1. The effect of generating two vortex rings could be achieved under other parameter conditions, with the exception of some parameter conditions when $D_1/D_2 = 4$. In most of the 277 sets of experiments, x_2 is greater than x_1. When $L_1/L_2 = 2.4$, $D_1/D_2 = 2$, $w_1 = 0.2$, x_1 reaches a maximum value of 13.7, and x_2 reaches a maximum value of 20 when $L_1/L_2 = 2$, $D_1/D_2 = 2.5$, $w_2 = 0.2$.
2. Within the parameter selection range of experiments and keeping other factors unchanged, when $D_1/D_2 < 4$, x_1 first increases and then decreases as w_1 increases, and x_2 first increases and then decreases as w_2 increases. When $D_1/D_2 = 4$, x_1 increases as w_1 increases, and x_2 decreases as w_1 increases.
3. The moving distance ratio x_1 first increases and then decreases as L_1/L_2 increases. When $D_1/D_2 < 4$, x_2 first increases and then decreases as L_1/L_2 increases. When $D_1/D_2 = 4$, x_2 decreases as w_2 increases when $L_1/L_2 = 2.4$ and $w_2 \geq 0.2$, $x_2 = 0$, which means that vortex ring 2 cannot be generated.
4. As D_1/D_2 increases, the moving distance ratio x_1 decreases while x_2 first increases and then decreases. When $D_1/D_2 = 4$, the generation effect of vortex rings is poor, and the moving distances x_1 and x_2 are both short.

There are still some limitations in our work, such as the experimental device is not precise enough, which leads to some errors in the experiment, and the research method is relatively single. In the future, more sophisticated experimental equipment will be used to measure some dynamic parameters of vortex rings. The characteristics of a reciprocating vortex ring generator will be studied using numerical simulation methods and compared with

experimental results. The reciprocating vortex ring generator will be multi-objective optimized to increase vortex rings' moving distance, etc.

ACKNOWLEDGEMENTS

The authors acknowledge financial support from the Postgraduate Research and Practice Innovation Project for Nanjing University of Aeronautics and Astronautics (No.xcxjh 20220215).

CONFLICT OF INTEREST

No potential conflict of interest was reported by the authors.

AUTHORS CONTRIBUTION

M. L. Zhou and **D. Han** designed the research. **M. L. Zhou** and **L. Zhu** conducted experiments. **S. Y. Yu** and **Y. F. Gao** processed the corresponding data. **M. L. Zhou** and **Q. L. Shi** wrote the first draft of the manuscript. **D. Han** and **W. F. He** helped to organize the manuscript.

REFERENCES

Buttà, P., & Marchioro, C. (2020). Time evolution of concentrated vortex rings. *Journal of Mathematical Fluid Mechanics*, *22*(2), 19. https://doi.org/10.1007/s00021-020-0482-x

Cao, Z., Wang, R., Zhai, C., Wang, Y., Zhao, T., & Wu, S. (2022). Flow characteristics and formation optimization of vortex ring air supply. *Indoor Air*, *32*(8), e13096. https://doi.org/https://doi.org/10.1111/ina.13096

Dabiri, J. O., & Gharib, M. (2004). Delay of vortex ring pinchoff by an imposed bulk counterflow. *Physics of Fluids*, *16*(4), L28-L30. https://doi.org/10.1063/1.1669353

Dasouqi, A. A., Yeom, G. S., & Murphy, D. W. (2020). Bursting bubbles and the formation of gas jets and vortex rings. *Experiments in Fluids*, *62*(1), 1. https://doi.org/10.1007/s00348-020-03089-0

Dipendra, G., Sanjay, P. S., & Jaywant, H. A. (2020). Design and development of a vortex ring generator to study the impact of the ring as a gust. *bioRxiv*, 2020.2010.2012.331777. https://doi.org/10.1101/2020.10.12.331777

Gemmell, B. J., Troolin, D. R., Costello, J. H., Colin, S. P., & Satterlie, R. A. (2015). Control of vortex rings for manoeuvrability. *Journal of The Royal Society Interface*, *12*(108), 20150389. https://doi.org/10.1098/rsif.2015.0389

Gharib, M., Rambod, E., & Shariff, K. (1998). A universal time scale for vortex ring formation. *Journal of Fluid Mechanics*, *360*, 121-140. https://doi.org/10.1017/S0022112097008410

Ikhlaq, M., Yasir, M., Ghaffari, O., & Arik, M. (2022). Acoustics and heat transfer characteristics of piezoelectric driven central orifice synthetic jet actuators. *Experimental Heat Transfer*, *35*(6), 758-779. https://doi.org/10.1080/08916152.2021.1946211

Jain, S., Sharma, S., Roy, D., & Basu, S. (2023). Vortical cleaning of oil-impregnated porous surfaces. *Physical Review Fluids*, *8*(4). https://doi.org/10.1103/PhysRevFluids.8.044701

Krueger, P. S. (2008). Circulation and trajectories of vortex rings formed from tube and orifice openings. *Physica D: Nonlinear Phenomena*, *237*(14), 2218-2222. https://doi.org/https://doi.org/10.1016/j.physd.2008.01.004

Limbourg, R., & Nedić, J. (2021a). An extension to the universal time scale for vortex ring formation. *Journal of Fluid Mechanics*, *915*. https://doi.org/10.1017/jfm.2021.141

Limbourg, R., & Nedić, J. (2021b). Formation of an orifice-generated vortex ring. *Journal of Fluid Mechanics*, *913*, A29, Article A29. https://doi.org/10.1017/jfm.2021.36

Maxworthy, T. (1977). Some experimental studies of vortex rings. *Journal of Fluid Mechanics*, *81*(3), 465-495. https://doi.org/10.1017/S0022112077002171

Mouallem, J., Daryan, H., Wawryk, J., Pan, Z., & Hickey, J. P. (2021). Targeted particle delivery via vortex ring reconnection. *Physics of Fluids*, *33*(10). https://doi.org/10.1063/5.0066443

New, T. H., Long, J., Zang, B., & Shi, S. (2020). Collision of vortex rings upon V-walls. *Journal of Fluid Mechanics*, *899*, A2, Article A2. https://doi.org/10.1017/jfm.2020.425

Nguyen, V. L., Takamure, K., & Uchiyama, T. (2019). Deformation of a vortex ring caused by its impingement on a sphere. *Physics of Fluids*, *31*(10), 107108. https://doi.org/10.1063/1.5122260

Noro, S., Suzuki, Y., Shigeta, M., Izawa, S., & Fukunishi, Y. (2013). Boundary layer receptivity to localized disturbances in freestream caused by a vortex ring collision. *Journal of Applied Fluid Mechanics*, *6*(3), 425-433. https://doi.org/10.36884/jafm.6.03.19484

Pullin, D. I. (1979). Vortex ring formation at tube and orifice openings. *The Physics of Fluids*, *22*(3), 401-403. https://doi.org/10.1063/1.862606

Ren, H., Zhang, G. X., & Guan, H. S. (2016). Numerical study of the instability and flow transition in a vortex-ring/wall interaction. *Journal of Applied Fluid Mechanics*, *9*(7), 2299-2309. https://doi.org/10.18869/acadpub.jafm.68.236.24926

Saaid, H., Segers, P., Novara, M., Claessens, T., & Verdonck, P. (2018). Single calibration multiplane stereo-PIV: the effect of mitral valve orientation on three-dimensional flow in a left ventricle model.

Experiments in Fluids, 59(3), 49. https://doi.org/10.1007/s00348-018-2504-5

Sakhri, N., Menni, Y., & Ameur, H. (2021). Enhancement of the natural ventilation within commercial and traditional wind towers in arid environments. *Journal of Applied Fluid Mechanics*, *14*(5),1329-1336. https://doi.org/10.47176/jafm.14.05.32153

Seth, D., Flammang, B. E., Lauder, G. V., & Tangorra, J. L. (2017). Development of a vortex generator to perturb fish locomotion. *Journal of Experimental Biology*, *220*(6), 959-963. https://doi.org/10.1242/jeb.148346

Shadden, S. C., Dabiri, J. O., & Marsden, J. E. (2006). Lagrangian analysis of fluid transport in empirical vortex ring flows. *Physics of Fluids*, *18*(4), 047105. https://doi.org/10.1063/1.2189885

Taddeucci, J., Peña Fernández, J. J., Cigala, V., Kueppers, U., Scarlato, P., Del Bello, E., & Panunzi, S. (2021). Volcanic vortex rings: axial dynamics, acoustic features, and their link to vent diameter and supersonic jet flow *Geophysical Research Letters*, *48*(15), e2021GL092899. https://doi.org/https://doi.org/10.1029/2021GL092899

Tan, J., Dong, P., Gao, J., Wang, C., & Zhang, L. (2023). Coupling bionic design and numerical simulation of the wavy leading-edge and seagull airfoil of axial flow blade for air-conditioner. *Journal of Applied Fluid Mechanics*, *16*(7),1316-1330. https://doi.org/10.47176/jafm.16.07.1634

Tian, H. Y., Xu, L., Hou, B. S., Huang, T., Huang, X. T., Liu, J. Q., & Wu, Y. J. (2021). Research on the feasibility verification based on continuous vortex ring generator and the matching degree of device parameters. *Journal of Physics: Conference Series*, *1888*(1). https://doi.org/10.1088/17426596/1888/1/012020

Wang, C., & Covington, J. A. (2023). The development of a simple projection-based, portable olfactory display device. *Sensors*, 23(11). https://doi.org/10.3390/s23115189

Wang, Y., Zhai, C., Cao, Z., & Zhao, T. (2020). Potential application of using vortex ring for personalized ventilation. *Indoor Air*, *30*(6), 1296-1307. https://doi.org/10.1111/ina.12699

Xia, X., Fu, C., Yang, Y., Yang, X., Gao, Y., & Qi, F. (2021). Vortex formation and frequency tuning of periodically-excited jet diffusion flames. *Proceedings of the Combustion Institute*, *38*(2), 2067-2074. https://doi.org/10.1016/j.proci.2020.08.015

Xia, X., & Zhang, P. (2018). A vortex-dynamical scaling theory for flickering buoyant diffusion flames. *Journal of Fluid Mechanics*, *855*, 1156-1169. https://doi.org/10.1017/jfm.2018.707

Xiang, Y., Qin, S., & Liu, H. (2018). Patterns for efficient propulsion during the energy evolution of vortex rings. *European Journal of Mechanics - B/Fluids*, 71,47-58. https://doi.org/https://doi.org/10.1016/j.euromechflu.2018.03.014

Yu, S., Han, D., He, W., Zhou, M., Zhu, L., Gao, Y., & Peng, T. (2023). Analysis and optimization of transient heat dissipation characteristics of high power resistors with a sensible heat storage method. *Applied Thermal Engineering*, *226*. https://doi.org/10.1016/j.applthermaleng.2023.120246

Zhai, C., Wang, Y., Cao, Z., Zhao, T., Wang, R., Zhang, C., & Wu, S. (2022). Effect of thermal buoyancy on vortex ring air supply mode. *Building and Environment*, *221*. https://doi.org/10.1016/j.buildenv.2022.109257

Zhang, X., Wang, J., & Wan, D. (2020). CFD investigations of evolution and propulsion of low speed vortex ring. *Ocean Engineering*, *195*, 106687. https://doi.org/https://doi.org/10.1016/j.oceaneng.2019.106687